Diffusion in concentrated lattice gases. VI. Tracer diffusion on two coupled linear chains

R. Kutner
*Institut für Festkörperforschung der Kernforschungsanlage Jülich, D-5170 Jülich, West Germany and Institute of Experimental Physics, University of Warsaw, Hoża 69, PL-00-681 Warszawa, Poland**

H. van Beijeren
Institut für Theoretische Physik A, Rheinisch-Westfälische Technische Hochschule Aachen, D-5100 Aachen, West Germany

K. W. Kehr
Institut für Festkörperforschung der Kernforschungsanlage Jülich, D-5170 Jülich, West Germany
(Received 16 April 1984)

Tagged-particle diffusion is investigated on a system of two coupled linear chains with an arbitrary ratio of the jump rates for jumps to unoccupied neighboring sites in the two principal directions. The mean-square displacement of a tagged particle is investigated both theoretically and by Monte Carlo simulations; the agreement between the results of these two approaches is found to be very satisfactory. Also the theoretical and simulated correlation factors, determining the coefficient of tracer diffusion, are always found to agree within a few percent. At small jump rate ratios, the mean-square displacement exhibits an intermediate t^{β} power-law behavior, with $\frac{1}{2}<\beta<1$, resulting from an incomplete changeover to a purely one-dimensional $t^{1/2}$ power law.

I. INTRODUCTION

It has been realized for some time that tracer diffusion on a one-dimensional array subject to a single filing constraint, which means that individual particles cannot pass each other, has anomalous character.[1-8] Specifically, the mean-square displacement of a tracer particle in such a system does not increase linearly with time for long times but only proportionally to $t^{1/2}$ and, accordingly, the tracer diffusion coefficient equals zero. However, as soon as the single filing constraint is relaxed, normal behavior of tracer diffusion is to be expected. A simple way to achieve this is by considering two coupled lines on which particles can pass each other by jumping from one line to the other.

A second motive for investigating such models is provided by lattice gases with anisotropic jump rates. Consider, for instance, a two-dimensional lattice gas with much larger jump rates in x direction than in y direction. A physical example could be a lattice gas on a surface with channels with short site distances, separated by larger distances. The diffusion of tagged particles should now exhibit one-dimensional effects on a intermediate time scale, and it is of interest to study the crossover to diffusional behavior at long times. Anisotropic lattice-gas models have been considered by Tahir-Kheli in two and three dimensions.[9] If one considers a two-dimensional lattice gas with periodic boundary conditions and introduces only two sites in the y direction, one again obtains the model of two coupled lines.

In this paper we will also consider this model. The specific properties of the lattice gas are defined in the following way: Each site can be either singly occupied or empty. Within each chain the particles can hop to empty neighboring sites with transition rate $\Gamma_{||}$; jumps to empty neighboring sites on the other chain occur with the rate $\Gamma_{\perp}$ in either direction (due to the periodic boundary conditions in the vertical direction this means that the actual jump rate between vertically neighboring sites equals $2\Gamma_{\perp}$). Besides the exclusion of jumps to occupied sites no further interactions between particles are considered.

As $\Gamma_{\perp}$ is increased from zero to finite values a changeover from single-filing behavior to normal diffusion occurs. A rough qualitative argument for the behavior of the tracer diffusion coefficient at small values of $\alpha=\Gamma_{\perp}/\Gamma_{||}$ can be given as follows: A tagged particle on a single chain experiences an averaged squared displacement according to the asymptotic law[7]

$$\langle x^2(t)\rangle=[2(1-c)/c](\Gamma_{||}t/\pi)^{1/2}\ .$$

Here c is the concentration, or average occupation number of the lattice gas, satisfying $0<c<1$. After a mean time $(2\Gamma_{\perp})^{-1}$ the particle will make a jump to the parallel chain and again start to diffuse according to the asymptotic law for a single chain. Repetition of this process leads to a mean-square displacement approximately

$$2\Gamma_{\perp}t[2(1-c)/c][\Gamma_{||}/(2\Gamma_{\perp}\pi)]^{1/2}\ ,$$

hence to a diffusion coefficient $D_t\sim\alpha^{1/2}\Gamma_{||}(1-c)/c$. This will be confirmed later by explicit calculations.

Apart from the diffusion coefficient the complete behavior of the mean-square displacement of a tagged particle as a function of time is of interest. On a single chain this quantity grows initially as t^1 and asymptotically assumes the $t^{1/2}$ behavior mentioned above. If the par-

ticle makes jumps between two such lines, another changeover from the single-chain behavior to diffusive behavior will occur. If $\alpha \ll 1$ this changeover simply appears as a changeover from $t^{1/2}$ to linear behavior. For slightly larger values of α, however, the changeover occurs at times where the $t^{1/2}$ behavior is not yet fully attained. It is then seen that the displacement behaves approximately like an intermediate power law t^{β} with $\frac{1}{2} < \beta < 1$ over one to two decades in time, and, of course, β approaches $\frac{1}{2}$ in the limit of very small α.

A changeover between $t^{1/2}$ and t behavior also occurs in other diffusion models. For instance, a lattice gas on a linear chain with periodic boundary conditions shows such a behavior.[10] Less understood is the occurrence of a $t^{-\beta'}$ term, with $\sim 1.3 < \beta' \leq 2$ in the velocity autocorrelation function of the two-dimensional Lorentz gas at moderate and high densities of scatterers, which was found by Alder and Alley in computer simulations.[11] Since the velocity autocorrelation function equals one-half times the second time derivative of the mean-square displacement,[10] this $t^{-\beta'}$ term implies the existence of a $t^{2-\beta'}$ term in the mean-square displacement. A plausible explanation seems to be that this term represents an intermediate-time behavior resulting from a changeover between short time and percolative behavior and another one between the latter and the asymptotic long-time behavior.

In Sec. II we develop a stochastic theory of tracer diffusion on two coupled lines that become exact in the limits of small vacancy or particle concentration. In the limit $\alpha = 0$, where the two lines decouple, this theory is slightly less accurate for general c than the theory presented in Ref. 10, but the extension to α values different from zero is straightforward, which is not the case with the latter theory. In Sec. III we present the results of numerical simulations and compare these to the theory of Sec. II as well as to Tahir-Kheli's theory.[9] Section IV contains our concluding remarks, along with a short discussion of the results on the two-dimensional Lorentz gas obtained by Alley and Alder.

II. VELOCITY AUTOCORRELATION FUNCTION AND MEAN-SQUARE DISPLACEMENT

The autocorrelation function of the tagged-particle velocity can be calculated by methods similar to those used in Ref. 10. Suppose the tagged particle performs jumps $\vec{p}_i$ at times t_i $(i=0,1,\ldots)$ with $0 \leq t_0 < t_1 < t_2 < \cdots$ and $\vec{p}_i = (p_{ix}, p_{iy}) \in \{(a,0), (-a,0), (0,a), (0,-a)\}$. Then the tagged-particle velocity is given as

$$\vec{v}(t) = \sum_{i=0}^{\infty} \vec{p}_i \delta(t - t_i) . \tag{1}$$

The velocity autocorrelation function is defined by

$$C(t) = \langle v_x(0) v_x(t) \rangle , \tag{2}$$

where we restrict ourselves to the x-x correlation function. The angular brackets denote a joint average over the equilibrium distribution of all particles at $t=0$ and over all realizations of the random hopping process for $t \geq 0$. From this the mean-square displacement follows directly as[10]

$$\langle [x(t) - x(0)]^2 \rangle = 2 \int_0^t dt' \int_0^{t'} dt'' \, C(t'') . \tag{3}$$

Inserting (1) into (2) we obtain the following expression for the velocity autocorrelation function:

$$C(t) = \left\langle \delta(t_0) \sum_{i=0}^{\infty} p_{0x} p_{ix} \delta(t - t_i) \right\rangle . \tag{4}$$

Here we used the fact that, in order to obtain a nonvanishing contribution, $v_x(0)$ has to be different from zero, hence the first jump of the tagged particle has to occur at $t=0$, and it has to be in the x direction as well. This has a probability density $2(1-c)\Gamma_{||}$, therefore the contribution to $C(t)$ from the $i=0$ term in the sum occurring in (4) is of the form

$$C^{(0)}(t) = 2(1-c)\Gamma_{||} a^2 \delta(t) . \tag{5}$$

To approximate the remaining terms in (4) we proceed in the following way: We call the vacancy with which the tagged particle exchanges positions at $x=0$ the *special vacancy*. If, right after the initial jump we would replace the special vacancy by an "average site" occupied with probability c and vacant with probability $1-c$, we would have on average a situation with complete mirror symmetry in the x direction about the tagged particle, and beyond (5) no further contributions to $C(t)$ would arise. This means that the nonvanishing contributions to $C(t)$ for $t>0$ result entirely from the difference in behavior between the special vacancy and the average site. To simplify the analysis of this difference we modify our definition of the microscopic dynamics in the following way:[12] we assume that each couple of neighboring sites in the horizontal, respectively, vertical direction, not containing the tagged particle, may exchange its contents at the constant exchange rates $\Gamma_{||}$ and $\Gamma_{\perp}$, respectively. The tagged particle, as before, may only exchange positions with a neighboring vacancy, at the rates $\Gamma_{||}$ and $\Gamma_{\perp}$ in the horizontal and vertical directions, respectively. So the difference with the original dynamics is that neighboring nontagged particles or vacancies may exchange positions, but this is immaterial to the dynamics of the tagged particle, since the latter does not distinguish the identities of the other particles.

The difference between the dynamics of special vacancy and average site can now be completely characterized by noting that the special vacancy performs a simple unconditional continuous time random walk, whereas the average site also performs a continuous time random walk, but under the condition that it can jump past the tagged particle only if it contains a vacancy.

A complication arises from the fact that the tagged particle also performs a hopping process, which is not simple to describe exactly. To approximate this we will assume that the tagged particle performs a simple continuous time random walk as well, with a vertical jump rate $(1-c)\Gamma_{\perp}$ and an effective horizontal jump rate $\Gamma_{||}^{f}$, which will be determined self-consistently from the long-time behavior of the tagged-particle mean-square displacement in the x direction. We will sometimes use the abbrevia-

tion b instead, defined by $\Gamma_{||}^{t}=b\Gamma_{||}$. The correlation factor is obtained by division with $1-c$,

$$f=\Gamma_{||}^{t}/[\Gamma_{||}(1-c)]=b/(1-c)\ . \tag{6}$$

The single line. It is instructive to calculate the velocity autocorrelation function for the simpler case of a single line first. Instead of $C(t)$ we rather consider its Laplace transform

$$\tilde{C}(s)=\int_0^\infty dt\, e^{-st}C(t)\ . \tag{7}$$

The self-correlation of the initial jump yields a contribution

$$\tilde{C}^{(0)}(s)=(1-c)\Gamma_{||}a^2\ . \tag{8}$$

After this initial jump, the first difference between the dynamics with the special vacancy and that with the average site occurs at the "first return" of the special vacancy, that is, when the special vacancy changes position with the tagged particle for the second time. The average site will do the same only with weight $1-c$, after which exactly the same situation occurs as when the special vacancy jumps. With the remaining weight c a particle remains positioned next to the special particle and no jump occurs. Let the probability density of a first return at time t after the initial jump at time 0 be $\psi(t)$ with Laplace transform $\tilde{\psi}(s)$. Then the noncompensated contribution to $\tilde{C}(s)$ from the first return of the special vacancy is

$$\tilde{C}^{(1)}(s)=-2(1-c)\Gamma_{||}a^2c\tilde{\psi}(s)\ . \tag{9}$$

To obtain the contribution resulting from the second return of the special vacancy one proceeds along similar lines. First one has to notice that only the noncompensated fraction c of the special vacancy contributes at this second return. Then, again, if right after the second return the special vacancy would be replaced by an average site no further contributions to $\tilde{C}(s)$ would result, and it is only the difference between the process involving the special vacancy and the one involving this new average site that contributes to $\tilde{C}(s)$. Hence a contribution of magnitude $2(1-c)\Gamma_{||}a^2[c\tilde{\psi}(s)]^2$ results. However, an additional term is to be subtracted from this, resulting from the situation where, with weight c, the first average site, filled with a particle, remains positioned next to the tagged particle when the special vacancy completes its first return. The occupation of all other sites follows the equilibrium distribution. This implies that the configuration of tagged particle and neighboring "average-site" particle can be subdivided according to the following symbolic equation:

$$\{\otimes\bullet\}=(1-c)\{\circ\otimes\bullet\}+c\{\bullet\otimes\bullet\}\ , \tag{10}$$

where $\otimes$ denotes the tagged particle, $\bullet$ an occupied site, and $\circ$ a vacancy. The factors $1-c$ and c denote the probabilities for the respective configurations. The second term on the right-hand side of (10) possesses mirror symmetry about the tagged particle, and hence will not contribute to $\tilde{C}(s)$. In a similar way the configuration occurring just after the first return of the special vacancy can be decomposed according to

$$\{\circ\otimes\}=c\{\circ\otimes\bullet\}+(1-c)\{\circ\otimes\circ\}\ . \tag{11}$$

Again, the second term on the right-hand side is mirror symmetric and does not contribute to $\tilde{C}(s)$. But the first configuration is precisely the same one occurring in the first term on the right-hand side of (10). Hence one may conclude that the term to be subtracted is just $(1-c)/c$ times the direct contribution from the second return of the special vacancy, and the total contribution from the second returns amounts to

$$\tilde{C}^{(2)}(s)=2(1-c)\Gamma_{||}a^2c(2c-1)\tilde{\psi}^2(s)\ . \tag{12}$$

Now it is simple to calculate the contribution from the nth return with the result

$$\tilde{C}^{(n)}(s)=(-1)^n2(1-c)\Gamma_{||}a^2c(2c-1)^{n-1}\tilde{\psi}^n(s)\ . \tag{13}$$

The full velocity autocorrelation function is found by summing over all n and is of the form

$$\tilde{C}(s)=(1-c)\Gamma_{||}a^2\frac{1-\tilde{\psi}(s)}{1+(2c-1)\tilde{\psi}(s)}\ . \tag{14}$$

Our next task is the calculation of $\tilde{\psi}(s)$, based on the random-walk assumptions for the special vacancy and tagged particle described above. The first step consists in expressing $\tilde{\psi}$ as

$$\tilde{\psi}(s)=\frac{\Gamma_{||}}{s+2\Gamma_{||}+\Gamma_{||}^{t}}\times\frac{1}{1-[(\Gamma_{||}+\Gamma_{||}^{t})/(s+2\Gamma_{||}+\Gamma_{||}^{t})]\tilde{X}(s)}\ . \tag{15}$$

Here $\Gamma_{||}/(s+2\Gamma_{||}+\Gamma_{||}^{t})$ is the contribution from a direct return after the initial jump; also see the Appendix for a more detailed treatment including transitions to the second line. The multiplicative factor sums a geometric series of contributions in which the basic building block consists of a jump bringing special vacancy and tagged particle two lattice units apart [with probability $(\Gamma_{||}+\Gamma_{||}^{t})/(s+2\Gamma_{||}+\Gamma_{||}^{t})$ in the Laplace regime], followed by a return to the situation where they are next to each other. The quantity $\tilde{X}(s)$ generally describes the first return probability for the distance between special vacancy and tagged particle from $(n+1)$, with $n\geq 1$, to n lattice units. It satisfies the algebraic equation[13]

$$\tilde{X}(s)=\frac{\Gamma_{||}+\Gamma_{||}^{t}}{[s+2(\Gamma_{||}+\Gamma_{||}^{t})]\{1-[(\Gamma_{||}+\Gamma_{||}^{t})/(s+2\Gamma_{||}+2\Gamma_{||}^{t})]\tilde{X}(s)\}}\ . \tag{16}$$

The solution of (16) is elementary. It can be written as

$$\tilde{X}=\frac{1+b+\zeta-\{\zeta[2(1+b)+\zeta]\}^{1/2}}{1+b} \tag{17}$$

with $\zeta=s/2\Gamma_{||}$. Substituting (17) into (15) and the latter equation into (14) one obtains a result for $\tilde{C}(s)$ in which only $\Gamma_{||}^{f}$ is unknown. The value of this quantity can be fixed now by imposing the self-consistency condition

$$\tilde{C}(0)=\Gamma_{||}^{f}a^2 . \tag{18}$$

In the case of the single line (18) immediately leads to $\Gamma_{||}^{f}=0$ as was to be expected,[7,10] but for the double line (18) will yield nonzero values for $\Gamma_{||}^{f}$.

The double line. In the case of the double line the first return of the special vacancy may occur either on the same line where the special particle is present, or on the other line. In the second case a situation arises where the tagged particle and special vacancy are found above each other. At least under the approximations adopted here, this situation on the average has perfect mirror symmetry about the axis through tagged particle and special vacancy, and hence, whatever happens afterwards, will, on the average, not contribute to the velocity autocorrelation function. On the other hand, if this first return happens with tagged particle and special vacancy on the same line, these two exchange positions and the analysis proceeds as in the case of a single line. This implies that (14) is still valid, provided that $\tilde{\psi}(s)$ is defined as the probability for a first return with tagged particle and special vacancy (or average site) on the same line. The calculation of $\tilde{\psi}(s)$ is straightforward but somewhat lengthy. Therefore, we defer it to an Appendix and merely quote the result

$$\tilde{\psi}(s)=\frac{\Gamma_{||}}{s+2\Gamma_{||}+\Gamma_{||}^{f}+2\gamma\Gamma_{||}}\left[1-\frac{1}{2}\frac{(\Gamma_{||}+\Gamma_{||}^{f})[\tilde{X}(s)+\tilde{X}(s+2\gamma\Gamma_{||})]}{s+2\Gamma_{||}+\Gamma_{||}^{f}+2\gamma\Gamma_{||}}\right.$$
$$\left.-\frac{\{2\gamma\Gamma_{||}+\frac{1}{2}(\Gamma_{||}+\Gamma_{||}^{f})[\tilde{X}(s)-\tilde{X}(s+2\gamma\Gamma_{||})]\}^2}{(s+2\Gamma_{||}+\Gamma_{||}^{f}+2\gamma\Gamma_{||})(s+2\gamma\Gamma_{||}+(\Gamma_{||}+\Gamma_{||}^{f})\{2-\frac{1}{2}[\tilde{X}(s)+\tilde{X}(s+2\gamma\Gamma_{||})]\})}\right]^{-1} \tag{19}$$

$$=\{\zeta+(1+b)+\gamma+\tfrac{1}{2}[\zeta(2+2b+\zeta)]^{1/2}+\tfrac{1}{2}[(\zeta+2\gamma)(2+2b+\zeta+2\gamma)]^{1/2}\}$$
$$\times(\zeta^2+(2+b)\zeta+(1+b)+(2\zeta+2+b)\{\gamma+\tfrac{1}{2}[\zeta(2+2b+\zeta)]^{1/2}+\tfrac{1}{2}[(\zeta+2\gamma)(2+2b+\zeta+2\gamma)]^{1/2}\}$$
$$+[\zeta(2+2b+\zeta)]^{1/2}\{2\gamma+[(\zeta+2\gamma)(2+2b+\zeta+2\gamma)]^{1/2}\})^{-1} . \tag{19'}$$

Here $\gamma=(2-c)\alpha$, with $\alpha=\Gamma_{\perp}/\Gamma_{||}$ as introduced in Sec. I, and $\tilde{X}(s)$ is given by (17). The correlation factor has to be determined by (18) and (6) again, which leads to the result

$$b=\frac{(1-c)(1+b)(\gamma+q)}{2c(1+b)+(2c+1+b)(\gamma+q)} \tag{20}$$

or

$$2cb(1+b)+[b^2+3cb-(1-c)](\gamma+q)=0 \tag{20'}$$

with $q=[\gamma(1+b+\gamma)]^{1/2}$. If, instead of solving for b in (20) one equalizes this quantity to $1-c$, substitutes this into the right-hand side of (20), and divides by $1-c$, one recovers Tahir-Kheli's expression for the correlation factor. In the limits $c\to 0$ and $c\to 1$ it coincides with our results, for intermediate concentrations, however, a self-consistent determination of b seems preferable.

For small s one can derive from (14) and (19) an expansion of $\tilde{C}(s)$ in powers of $\sqrt{\zeta}$ in the form

$$\tilde{C}(s)=\Gamma_{||}a^2(b+c_1\sqrt{\zeta}+c_2\zeta+\cdots) . \tag{21}$$

The coefficients c_1 and c_2 are given by

$$c_1=c(1-c)[2(1+b)]^{1/2}\left[\frac{2c(1+b)-(1+b-2c)(\gamma+q)}{4c^2(1+b)-(1+b-2c)(1+b+2c)\gamma}\right]^2 ,$$
$$c_2=(1-c)b\left[\frac{b_2-a_2}{b_0-a_0}+\frac{b_1^2-b_0b_2+(2c-1)(2a_1b_1-a_0b_2-a_2b_0)+(2c-1)^2(a_1^2-a_0a_2)}{[b_0+(2c-1)a_0]^2}\right] , \tag{22}$$

with $a_0=1+b+\gamma+q$,

$$a_1=\left[\frac{1+b}{2}\right]^{1/2},$$

$$a_2=1+\frac{(1+b+2\gamma)q}{4\gamma(1+b+\gamma)},$$

$$b_0=1+b+(2+b)(\gamma+q),$$

$$b_1=(2+b)\left[\frac{1+b}{2}\right]^{1/2}+2[2(1+b)(\gamma+q)]^{1/2},$$

$$b_2=(2+b)+2(\gamma+q)+\frac{(2+b)(1+b+\gamma)q}{4\gamma(1+b+\gamma)}.$$

III. COMPARISON WITH NUMERICAL SIMULATIONS

The numerical calculations were made partly on an IBM 370/148 computer in Warsaw, and partly on an IBM 3033 computer at Jülich. The simulation of the hopping process of the particles on the two coupled chains was made by standard Monte Carlo techniques which have been comprehensively described in Ref. 14 for the case of tracer diffusion in an fcc lattice gas. In this paragraph some special features of the procedure used for our model are presented. Lattices with at least 1000×2 sites were introduced and periodic boundary conditions imposed. Some runs were made with reflecting boundary conditions in the x direction to verify the independence of the results from the boundary conditions. The lattices were randomly occupied by particles with prescribed average concentration c.

For a given ratio $\alpha=\Gamma_\perp/\Gamma_{||}$ the hopping process was simulated in the following way. First, a particle was selected at random. Second, a random number ξ with $0<\xi\leq1$ was generated. If $0<\xi\leq[2(1+\alpha)]^{-1}$ a jump in positive direction was attempted, if $[2(1+\alpha)]^{-1}<\xi\leq(1+\alpha)^{-1}$ a jump in negative direction was attempted, and if $(1+\alpha)^{-1}<\xi\leq1$ a jump in the y direction was attempted. Jumps were executed when the final site was unoccupied. This process was repeated many times. In such simulations, time is usually measured in Monte Carlo steps (MCS) per particle which are defined as the average number of attempted jumps per particle. This corresponds to setting $2\Gamma_{||}+2\Gamma_\perp=1$. Here we prefer the total jump rate $2\Gamma_{||}$ in x direction as the inverse time unit. This requires rescaling of the time scale in MCS by a factor $(1+\alpha)^{-1}$. Further details of the numerical procedure can be found in Ref. 14.

The results of the simulations for three different concentrations are given in Figs. 1–3, together with the predictions of the theory. Four different ratios α of the perpendicular to the parallel jump rates were used (five for the largest concentration), and also tracer diffusion on a single line, corresponding to $\alpha=0$ was simulated. These simulations cover times between 1 and 10^4 [in units of $(2\Gamma_{||})^{-1}$], and relatively small particle numbers were used, except at the largest concentration. The theoretical curves for finite α were obtained by numerical inverse Laplace transformation of Eqs. (14) and (19), and the inversion routine of Honig and Hirdes[15] was used. One notes very good agreement between theory and simulations. The agreement is especially satisfactory at the highest concentration $c=0.972$; remember that the theory becomes exact in the limit $c\to1$.

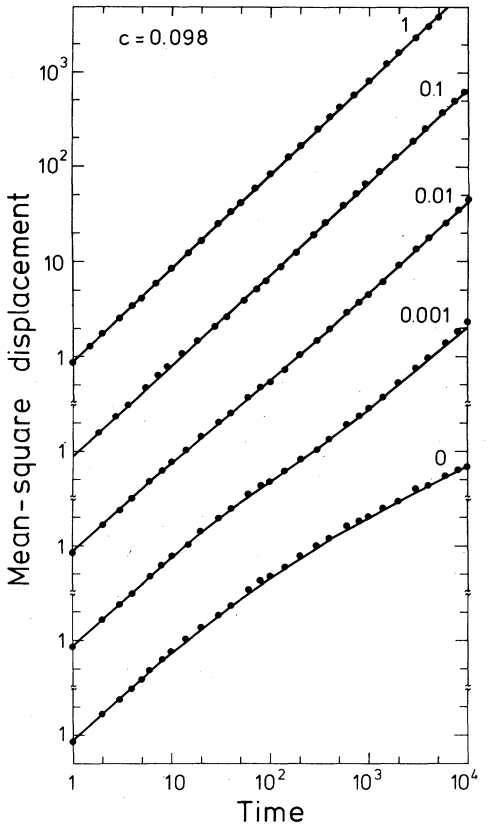

FIG. 1. Mean-square displacement of tagged particles on two coupled linear chains. Solid lines: theory; closed circles: results of the numerical simulations with two chains with 20000 sites and 1965 particles together. The ratio α of the perpendicular to the parallel jump rate is indicated to the right. For $\alpha=0$ one line with the same number of sites and particles was used. Time is given in units of $(2\Gamma_{||})^{-1}$.

The theoretical curves for the single line were obtained by inversion of Eq. (14) where Eqs. (15) and (17) with $\Gamma^f_{||}=0$ were used. [This is equivalent to setting $\alpha=0$ in Eq. (19)]. Comparison with the simulated points shows satisfactory agreement. In Ref. 10 a slightly more refined theory for the single line has been developed. On comparing this theory with the numerical data, somewhat better agreement is found. However, the differences between both theories are at most a few percent in the intermediate-time regime. In the short- and long-time regions both theories yield identical results.

The qualitative behavior of the curves with finite α is as expected from the discussion in the Introduction: The initial rise of the mean-square displacement is followed by an intermediate behavior proportional to t^β and finally the diffusive behavior, proportional to t^1, is approached. There is a point of inflection in the curves $\ln\langle x^2(t)\rangle$

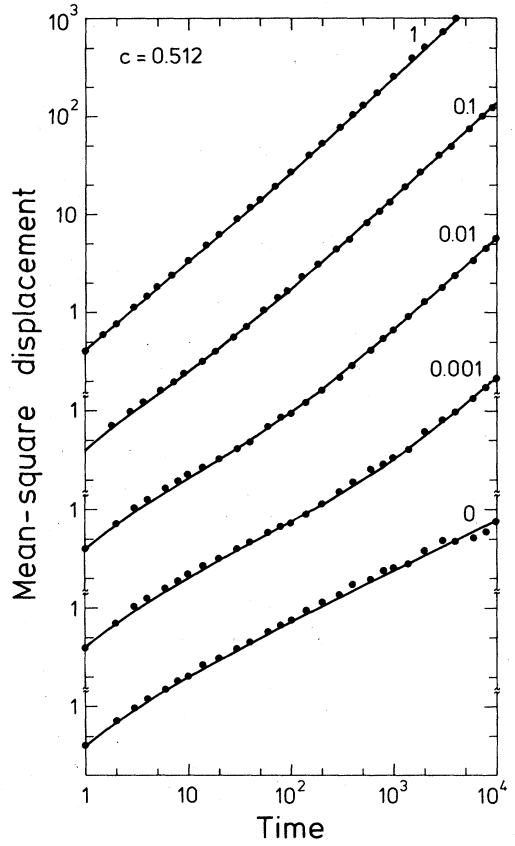

FIG. 2. Mean-square displacement of tagged particles on two coupled linear chains. 4000 sites and 2049 particles were used in the simulations. Further details are given in Fig. 1.

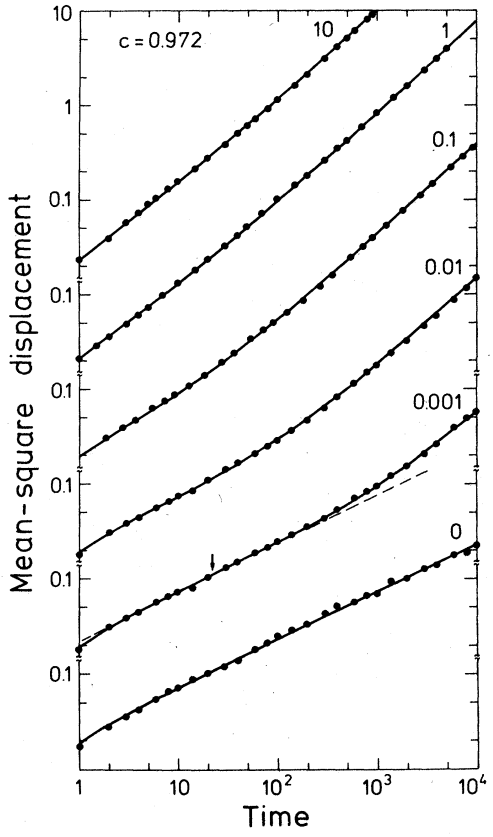

FIG. 3. Mean-square displacement of tagged particles on two coupled linear chains. 12 800 sites and 12 439 particles were used in the simulations. Further details are given in Fig. 1; the arrow and the dashed line are explained in the main text.

versus ln$t$. If true power-law behavior would apply, the derivative

$$\left[t\frac{d}{dt}\right]^2 \ln\langle x^2(t)\rangle \tag{23}$$

would be identically zero in the corresponding range. In fact, this derivative vanishes at one point only, marked in Fig. 3 by an arrow for $\alpha=0.001$. We have determined the apparent exponent of an assumed power-law behavior near the inflection point from (14) and (19), for $c=0.972$; this exponent is displayed in Fig. 4 as a function of α. For $\alpha\gg 1$ the exponent β approaches the value $\beta=0.808\cdots$. This means that the graph $\ln\langle x^2(t)\rangle$ versus ln$t$ always has an inflection point and that the mean-square displacement is different at short and long times in the limit of large α. In both limiting regions it is proportional to t^1, but with different coefficients. These coefficients, which are twice the diffusion coefficients for infinite and zero frequency for short and long times, respectively, are given by $(1-c)\Gamma_{||}a^2$ at short times and by $(1-c)\Gamma_{||}a^2/3$ for long times and $c\to 1$. The correlation factor $f=\frac{1}{3}$ is easily understood by considering $\langle\cos\theta\rangle$ for a tagged particle in the limits $\alpha\to\infty$ and $c\to 1$. Since in this limit the special vacancy hops rapidly between the two lines, it exchanges with probability $\frac{1}{2}$ with the tagged particle, and with the same probability with the corresponding particle on the other line. Hence $\langle\cos\theta\rangle=-\frac{1}{2}$ and $f=\frac{1}{3}$. This value of the correlation factor is consistent with the results presented in Fig. 3. We refrain from extending these considerations to other concentrations.

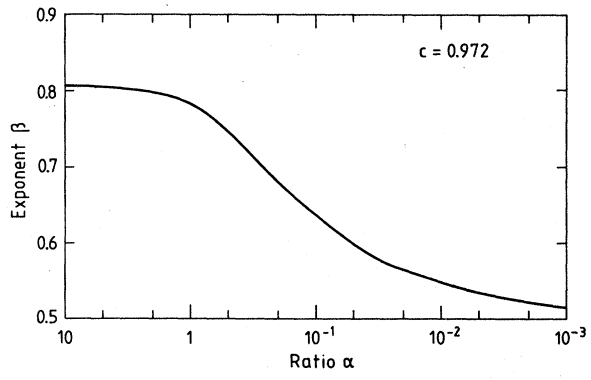

FIG. 4. Apparent exponent of the intermediate power-law behavior of the mean-square displacement as a function of the ratio of perpendicular to parallel jump rate.

For $\alpha \to 0$ the exponent approaches $\frac{1}{2}$ as expected. The dashed line in Fig. 3 indicates the power-law behavior for $c=0.972$ and $\alpha=0.001$; this behavior is followed by the mean-square displacement over approximately two decades. However, this is a relatively favorable case, for larger α and lower concentrations c the apparent power-law behavior is less pronounced. We stress that the apparent power-law behavior is an intermediate phenomenon, caused by the interplay between the changeover from t^1 to $t^{1/2}$ in the linear chain, and the changeover from $t^{1/2}$ to t^1 behavior in the coupled system.

While the theory for our model is exact in the limits $c \to 1$ and $c \to 0$, it is an approximation for intermediate c. In order to more closely examine the quality of the approximation, we have performed a simulation at $c=0.499$ and $\alpha=0.01$ with 19 940 particles, up to 5×10^3 time units, see Fig. 5. The agreement of the simulations with the theory is quite good, although there seems to be a small yet systematic difference. The figure also indicates the theory of Tahir-Kheli obtained by setting $b=1-c$ in (19); it is apparently a less accurate approximation.

The results presented up to now give the mean-square displacement normally up to 10^4 time steps. For smaller α and larger c the asymptotic diffusional behavior is barely reached. To determine the coefficient of tracer diffusion more accurately, we have also performed simulations at 11 different concentrations up to 10^5 time units, with typically 2000 particles (3113 at the largest concentration) and $\alpha=0.01$. We extracted the diffusion coefficient by fitting the data to the following asymptotic behavior:

$$\langle x^2(t)\rangle = (1-c)ft + \frac{2c_1}{\sqrt{\pi}} t^{1/2} + c_2 \,. \tag{24}$$

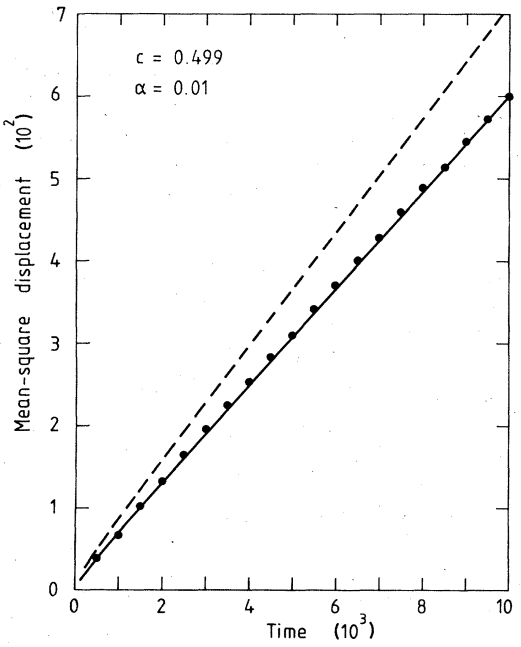

FIG. 5. Mean-square displacement of tagged particles on two coupled linear chains. Solid line: our theory; dashed line: theory of Tahir-Kheli; closed circles: results of the simulations with 40 000 sites and 19 940 particles together.

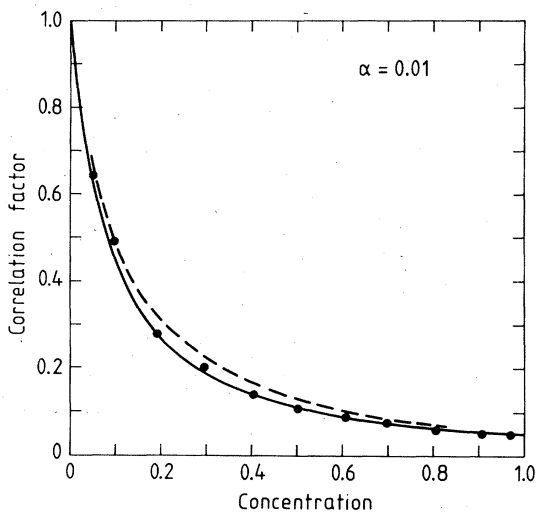

FIG. 6. Correlation factor as a function of concentration for the ratio $\alpha=0.01$. Solid line: our theory; dashed line: theory of Tahir-Kheli (Ref. 9); solid circles are the results of the simulations.

This ansatz is equivalent to Eq. (21); the rate $\Gamma_{||}$ has been put equal to $\frac{1}{2}$. In the actual fit, the logarithm of the theory function (24) was compared with the logarithm of the simulation values. This procedure is reasonable, since the scatter of the data points grows roughly with t, i.e., the relative scatter is constant. The results for $f(c)$ are given in Fig. 6, together with the theoretical values for $f(c)$ resulting from the implicit equation (20). The figure also contains the theory for $f(c)$ of Tahir-Kheli.[9] One notes better agreement with the theory given here. However, there remain discrepancies between this theory and the simulations for $c \lesssim 0.5$. It is not clear as to how far these result from the inherent inaccuracies of the simulations and how far they are due to the approximations made in the theory. Simulations with larger particle numbers up to 10^5 time steps would be desirable, however, the time consumption would be prohibitive with the present, conventional simulation techniques.

The results for the parameter c_1 for $\alpha=0.01$ are shown in Fig. 7, together with the theoretical curve representing Eq. (22). There is considerable scatter in the values of this parameter, and some dependence on the fitting procedure. The tendency of the theoretical curve is well recognized in the data. Again, the quality of the results could be improved by using larger particle numbers, but we were not willing to bear the corresponding costs in computing time.

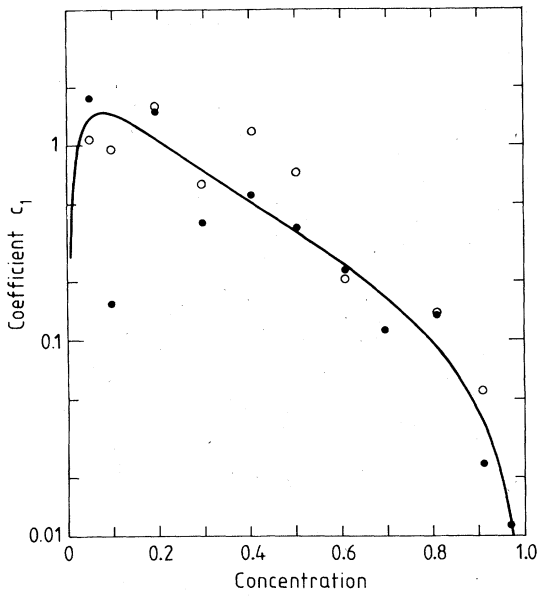

FIG. 7. Coefficient c_1 of the first correction to the asymptotic behavior of the mean-square displacement. Solid line: theory; closed circles: two-parameter fit ($c_2=0$) of simulated mean-square displacement with Eq. (24); open circles: three-parameter fit.

IV. DISCUSSION

The Monte Carlo simulations reported in Sec. III confirm the accuracy of the theory developed in Sec. II of this paper; for all the parameter values investigated the discrepancies between theoretical and computed values of the mean-square tagged-particle displacement over the whole time region never exceed a few percent. Tahir-Kheli's theory[9] also yields fair agreement with our Monte Carlo results, but not quite as good as the theory developed here. The differences between the two theories show up most clearly at concentrations close to $c=\frac{1}{2}$, in the limits $c\to 0$ and $c\to 1$ both theories become exact. In the limit of vanishing jump rate ratio α, where both lines decouple, the theory of Sec. II is slightly worse than the theory developed in Ref. 10, however, the latter cannot be generalized straightforwardly to the case of a nonzero α.

For small α the mean-square displacement as a function of time clearly exhibits the two expected changeovers: one from short-time t^1 behavior to the $t^{1/2}$ behavior characteristic of single file diffusion, and one from the $t^{1/2}$ behavior to the asymptotic diffusive t^1 behavior. However, unless the jump-rate ratio really is very small ($\alpha<0.001$), the intermediate-time behavior does not really follow a $t^{1/2}$ power law, but rather an approximate t^{β} power with $\frac{1}{2}<\beta<1$. The range over which this approximate intermediate power law persists increases with decreasing α. For $c=0.972$ and $\alpha=0.001$ it extends over more than two decades in time.

Similar intermediate power laws have been found numerically by Alder and Alley[11] for the velocity autocorrelation of the two-dimensional Lorentz gas. For the case of overlapping scatterers, where, as a function of scatterer density, a percolation transition is known to occur, they find a changeover from the theoretically predicted t^{-2} behavior at low scatterer density to a $t^{-\beta'}$ power-law decay with $\beta'\approx 1.33$ at densities near the percolation density, followed by a decrease of β' with further increase of the scatterer density. Just as our intermediate t^{β} power law for the mean-square displacement resulted from an incomplete changeover to single filing behavior, the $t^{-\beta'}$ power law of Alley and Adler can be understood to result from an incomplete changeover to percolative behavior. The maximal value of $\beta'\approx -1.33$ is in good agreement with theoretical predictions for the percolation point.[16–18] Unfortunately, their molecular-dynamics simulations could not be extended to long enough times to see the asymptotic behavior following this intermediate power law. Their results for nonoverlapping scatterers, where no percolation transition exists, except at perfect close packing, are consistent with this picture: There the low density t^{-2} behavior changes to $t^{-\beta'}$ behavior with β' increasing with density over the investigated range of scatterer densities. Whether β' approaches the percolation value at the close-packing density cannot be concluded with certainty, however.

Further, we want to mention that the theory developed in Sec. II can be extended straightforwardly to simple cubic lattices with or without periodicity, in an arbitrary number of dimensions. This will be the subject of a planned forthcoming paper. Presumably, extension to more complicated lattices can also be made without problems. Finally, the coefficient of the $t^{1/2}$ term in the asymptotic expansion for large times can be compared to mode-coupling predictions.[19] This too is presently under investigation.

ACKNOWLEDGMENTS

One of the authors (R.K.) was partially supported by Contract No. MR.I.5/K-8.6.01 of Warsaw University.

APPENDIX: DERIVATION OF $\tilde{\psi}(s)$

For calculating the probability of a first return with tagged particle and special vacancy on the same line, first notice that before this return the relative motions in the horizontal and vertical directions are completely independent of each other. We want to ignore correlations between subsequent vertical jumps of the tagged particle; for the special vacancy such correlations are not present. Let $p_+(t)$ be the probability to find tagged particle and special vacancy on the same line at time t, and $p_-(t)$ the probability to find them on different lines. These quantities satisfy the differential equations

$$\frac{d}{dt}p_+(t)=2\Gamma_\perp(2-c)[p_-(t)-p_+(t)]\,,$$
$$\frac{d}{dt}p_-(t)=2\Gamma_\perp(2-c)[p_+(t)-p_-(t)]\,. \tag{A1}$$

The solution, with initial conditions $p_+(0)=1$ and $p_-(0)=0$, is found as

$$p_{\pm}(t)=\tfrac{1}{2}\{1\pm\exp[-4\Gamma_{\perp}(2-c)t]\}$$
$$=\tfrac{1}{2}[1\pm\exp(-4\gamma\Gamma_{||}t)]\ . \qquad \text{(A2)}$$

From (A1) and (A2) it follows that the Laplace-transformed probability density for a first return of the relative distance in the x direction between tagged particle and special vacancy from $n+1$ to n, with $n\geq 1$, can be described as

$$\tilde{Y}_{\pm}(s)=\tfrac{1}{2}[\tilde{X}(s)\pm\tilde{X}(s+4\gamma\Gamma_{||})]\ , \qquad \text{(A3)}$$

where the plus sign refers to a return where tagged particle and special vacancy are both initially and finally either on the same line or on different lines, and where the minus sign refers to situations where tagged particle and special vacancy are either initially on the same line and finally on different lines, or just the other way around.

Next we have to consider what may happen if tagged particle and special vacancy are just one lattice unit apart in the x direction. If they are on the same line they may either exchange positions, with jump rate $\Gamma_{||}$; they may move two lattice units apart in the x direction, with jump rate $\Gamma_{||}+\Gamma_{||}^{f}$, or either of them may jump in the y direction, with jump rate $2\gamma\Gamma_{||}$. The respective waiting-time distributions for these three processes are

$$\Gamma_{||}\exp[-(2\Gamma_{||}+\Gamma_{||}^{f}+2\gamma\Gamma_{||})t]\ ,$$
$$(\Gamma_{||}+\Gamma_{||}^{f})\exp[-(2\Gamma_{||}+\Gamma_{||}^{f}+2\gamma\Gamma_{||})t]\ ,$$

and

$$2\gamma\Gamma_{||}\exp[-(2\Gamma_{||}+\Gamma_{||}^{f}+2\gamma\Gamma_{||})t]\ .$$

If the two are on different lines they may jump above each other, with jump rate $\Gamma_{||}+\Gamma_{||}^{f}$, away from each other, with the same jump rate, and next to each other, with jump rate $2\gamma\Gamma_{||}$. The respective waiting-time distributions accordingly are given as

$$(\Gamma_{||}+\Gamma_{||}^{f})\exp[-2(\Gamma_{||}+\Gamma_{||}^{f}+\gamma\Gamma_{||})t]$$

and

$$2\gamma\Gamma_{||}\exp[-2(\Gamma_{||}+\Gamma_{||}^{f}+\gamma\Gamma_{||})t]\ .$$

Now for the first return probability on the same line we can set

$$\tilde{\psi}(s)=[1-\tilde{Y}(s)]^{-1}\frac{\Gamma_{||}}{s+2\Gamma_{||}+\Gamma_{||}^{f}+2\gamma\Gamma_{||}}\ . \qquad \text{(A4)}$$

The factor $\Gamma_{||}/(s+2\Gamma_{||}+\Gamma_{||}^{f}+2\gamma\Gamma_{||})$ is the exchange probability when tagged particle and special vacancy are positioned next to each other, and $\tilde{Y}(s)$ describes the probability of a first return to this situation under the conditions that tagged particle and/or special vacancy move before exchanging positions, and before returning next to each other do not move through positions above each other. The factor $(1-\tilde{Y})^{-1}$ results from the summation of an infinite geometric series. For $\tilde{Y}(s)$ we obtain the following explicit expression:

$$\tilde{Y}(s)=\frac{\Gamma_{||}+\Gamma_{||}^{f}}{s+2\Gamma_{||}+\Gamma_{||}^{f}+2\gamma\Gamma_{||}}\tfrac{1}{2}[\tilde{X}(s)+\tilde{X}(s+4\gamma\Gamma_{||})]$$
$$+\left[\frac{2\gamma\Gamma_{||}}{s+2\Gamma_{||}+\Gamma_{||}^{f}+2\gamma\Gamma_{||}}+\frac{\Gamma_{||}+\Gamma_{||}^{f}}{s+2\Gamma_{||}+\Gamma_{||}^{f}+2\gamma\Gamma_{||}}\tfrac{1}{2}[\tilde{X}(s)-\tilde{X}(s+4\gamma\Gamma_{||})]\right]$$
$$\times\left[1-\frac{\Gamma_{||}+\Gamma_{||}^{f}}{s+2(\Gamma_{||}+\Gamma_{||}^{f})+2\gamma\Gamma_{||}}\tfrac{1}{2}[\tilde{X}(s)+\tilde{X}(s+4\gamma\Gamma_{||})]\right]^{-1}$$
$$\times\left[\frac{2\gamma\Gamma_{||}}{s+2(\Gamma_{||}+\Gamma_{||}^{f})+2\gamma\Gamma_{||}}+\frac{\Gamma_{||}+\Gamma_{||}^{f}}{s+2(\Gamma_{||}+\Gamma_{||}^{f})+2\gamma\Gamma_{||}}\tfrac{1}{2}[\tilde{X}(s)-\tilde{X}(s+4\gamma\Gamma_{||})]\right]\ . \qquad \text{(A5)}$$

Here the first term on the right-hand side contains the contributions from a jump in the x direction, followed by a first return to the neighboring configuration. In the second contribution the term $2\gamma\Gamma_{||}/(s+2\Gamma_{||}+\Gamma_{||}^{f}+2\gamma\Gamma_{||})$ describes the effect of a single vertical jump and the other term between the first large parentheses describes a horizontal jump, followed by a return to neighboring positions on different lines. The factor between the next pair of large parentheses sums the contributions of additional returns to neighboring positions on different lines. Finally, the factor in the last pair of large parentheses describes the probability for a return to neighboring positions on the same line, either through a single vertical jump, or through a horizontal jump followed by a return in which tagged particle and special vacancy have joined the same lines. Substitution of (A5) into (A4) immediately leads to (19).

*Permanent address.

[1]E. J. Harris, *Transport and Accumulation in Biological Systems* (Butterworths, London, 1960).

[2]E. J. A. Lea, J. Theor. Biol. 5, 102 (1963).

[3]K. Heckmann, in *Passive Permeability of Cell Membranes, Biomembranes,* edited by F. Kreuzer and J. F. G. Segers (Plenum, New York, 1972), Vol. 3, p. 127.

[4]T. E. Harris, J. Appl. Prob. 2, 323 (1965).

[5]F. Spitzer, Adv. Math. **5**, 246 (1970); R. Arratia, Ann. Prob. **11**, 362 (1983).
[6]P. M. Richards, Phys. Rev. B **16**, 2011 (1978).
[7]P. A. Fedders, Phys. Rev. B **17**, 40 (1978).
[8]S. Alexander and P. Pincus, Phys. Rev. B **18**, 2011 (1978).
[9]R. A. Tahir-Kheli, Phys. Rev. B **27**, 6072 (1983).
[10]H. van Beijeren, K. W. Kehr, and R. Kutner, Phys. Rev. B **28**, 5711 (1983).
[11]B. J. Alder and W. E. Alley, J. Stat. Phys. **19**, 341 (1978); in *Studies in Statistical Mechanics,* edited by H. J. Raveché (North-Holland, Amsterdam, 1981), Vol. IX; W. E. Alley, Ph.D. thesis, University of California—Livermore, 1979 [Report No. UCRL-52815 (unpublished)].
[12]The type of special vacancy dynamics defined here is distinctly different from that adapted in Ref. 10. The latter is slightly better for the single file case, but cannot be adapted easily to diffusion on two coupled lines.
[13]M. H. Ernst and H. van Beijeren, J. Stat. Phys. **26**, 1 (1981).
[14]K. W. Kehr, R. Kutner, and K. Binder, Phys. Rev. B **23**, 4931 (1981).
[15]G. Honig and U. Hirdes, J. Comput. Appl. Math. **10**, 113 (1984).
[16]W. Götze, E. Leutheuser, and S. Yip, Phys. Rev. A **23**, 2634 (1981).
[17]A. Masters and T. Keyes, Phys. Rev. A **26**, 2129 (1982).
[18]Y. Gefen, A. Aharony, and S. Alexander, Phys. Rev. Lett. **50**, 77 (1983).
[19]H. van Beijeren, J. Stat. Phys. **32**, 399 (1984).